

High Yield Preparation Method of Thermally Stable Cellulose Nanofibers

Yuanyuan Li, Hongli Zhu, Mei Xu, Zhiliang Zhuang, Mengdie Xu, and Hongqi Dai *

The preparation of nanocellulose fibers (NFs) is achieved through pretreating cellulose in a NaOH/urea/thiourea solution, and then defibrillating the fibers through ultrasonication, resulting in a high yield of 85.4%. Extensive work has been done to optimize the preparation parameters. The obtained NFs are about 30 nm in diameter with cellulose II crystal structure. They possess high thermal stability with an onset of thermal degradation at 270 °C and a maximum degradation temperature of 370 °C. Such NFs have potential applications in transistors and batteries with high thermal stability. NFs-H were obtained by homogenizing undefibrillated fibers separated from the preparation of NFs. NFs-H were also in cellulose II crystal form but with lower thermal stability due to low crystallinity. They can be applied to make highly transparent paper.

Keywords: Nanocellulose fibers; High yield; Thermal stability; Ultrasonication; Cellulose II

Contact information: College of Light Industry Science and Engineering, Nanjing Forestry University, Nanjing, Jiangsu 210037, P. R. China; * Corresponding author: hgdhq@njfu.edu.cn

INTRODUCTION

Cellulose is considered to be the most suitable precursor for environmentally friendly and renewable materials due to its green nature and inexhaustibility. Nanosized cellulose particles (NCs), prepared by processing a variety of raw cellulose materials, has gained increasing attention (Martinez-Sanz *et al.* 2011; Mishra *et al.* 2011; Zhu *et al.* 2013). They show impressive mechanical properties, excellent reinforcing capabilities, low weights, and low coefficients of thermal expansion, making them useful in a variety of applications, including reinforcing agents, functional films, texturing agents, and templates (Fox *et al.* 2012; Hu *et al.* 2013; Korhonen *et al.* 2011; Nogi *et al.* 2009; Zhu *et al.* 2013).

NCs basically consist of cellulose nanocrystals, nanofibrillated cellulose, and bacterial cellulose. There are different approaches to make NCs, including homogenization, microfluidization, micro-grinding, cryocrushing, acid hydrolysis, and TEMPO ((2,2,6,6-tetramethylpiperidin-1-yl)oxidanyl) oxidation, or their combination (Beck-Candanedo *et al.* 2005; Chen *et al.* 2011; Li and Dai, 2012; Lavoine *et al.* 2012; Li *et al.* 2013). A main problem with nanocellulose preparation through chemical methods is poor yield (Tang *et al.* 2011). The maximum yield of NCs obtained through acid hydrolysis is usually lower than 50% (Beck-Candanedo *et al.* 2005; Bondeson *et al.* 2006; Tang *et al.* 2011). Sadeghifar *et al.* (2011) produced cellulose nanocrystals using hydrobromic acid (HBr) with a yield of 70% under the conditions of 2.5 M HBr, a reaction temperature at 100 °C, and sonication time of 3 h. Recently, Wang *et al.* (2012) obtained a high yield of cellulose nanocrystals by simultaneous recovery of cellulosic

solids residues. Another way to obtain NCs with high yield is mechanical treatment. However, such an approach faces problems of high energy consumption (Spence *et al.* 2011). Mechanical, chemical, and enzymatic pretreatments are used to disintegrate fibers or to swell the fibers prior to the mechanical treatment with the aim of reducing energy consumption (Li *et al.* 2011). Mechanical treatments such as refining, PFI milling, and Valley beating remove the primary cell wall and expose the more organized fibrils located in the secondary cell wall for further processing (Montanari *et al.* 2005). The introduction of charged groups onto the surface of the fibers by chemical reaction leads to the appearance of repulsive forces that also weaken the structure (Isogai *et al.* 2011). When a sufficient amount of charged groups were introduced to fibers (≥ 3 millimoles of COO per gram of dried fibers), a maximum of 50 to 60 wt% of the original cellulose was converted into NFs (Tejado *et al.* 2012). A mild enzymatic treatment is observed to increase the swelling of cellulosic pulp fiber, thus facilitating the production of NFs (Henriksson *et al.* 2007).

The thermal stability of NCs is usually lower than that of micro-sized pure cellulose fiber due to the smaller fiber dimension, which leads to higher surface areas exposed to heat (Jiang and Hsieh 2013; Yue 2011). Most NCs are in the cellulose I form, and usually the onset thermal degradation temperature of NCs is below 255 °C (Lu and Hsieh 2010; Martinez-Sanz *et al.* 2011; Martins *et al.* 2011). This restricts the application of NCs to a relatively low temperature. Cellulose II has been considered as the most thermodynamically stable structure, since the chains are in an antiparallel arrangement (Habibi *et al.* 2010). Recently, a mixture of sodium hydroxide (NaOH)/thiourea, NaOH/urea, and NaOH/thiourea/urea aqueous solutions were used to “dissolve” cellulose, obtaining cellulose in the cellulose II crystalline arrangement. In the cellulose solution, there exists a synergic interaction of NaOH and urea/thiourea. The NaOH acts to “hydrate” the hydroxyl groups within the fibers, leading to swelling of the fibers (Yan and Gao 2008). Based on this idea, we made high thermally stable cellulose II NFs by first swelling the fibers in a NaOH/urea/thiourea pretreatment system and then isolating the NFs through ultrasonication. After centrifugation, large fibers were separated from the NFs. The large fibers were collected for further homogenization (Fig. 1).

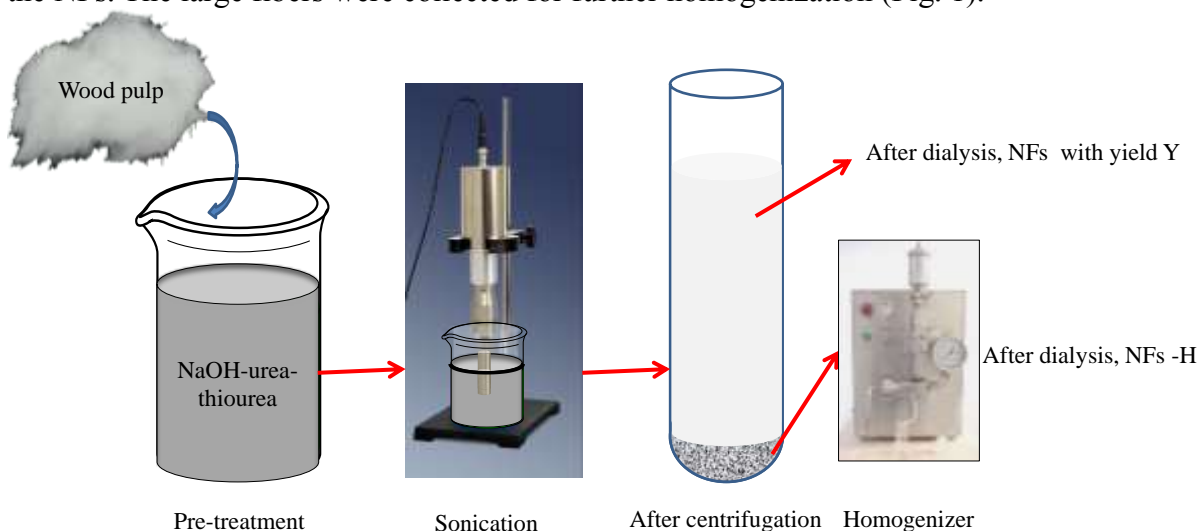


Fig. 1. Schematic to show NFs preparation

These cellulose nanofibers obtained by the further homogenization were named NFs-H. The theoretical yield of NFs and NFs-H is 100%, since only swelling and mechanical defibrillation happens. The NFs having high thermal stability have potential application in making films for electronic devices that need thermal stability under high temperature, such as separators for batteries. NFs-H has lower thermal stability but can be potentially applied in transparent paper fabrication.

EXPERIMENTAL

Materials

The bleached softwood kraft pulp was supplied by Suzano, SP, Brazil in dry sheet form. The pulp was beaten in a Valley beater to 150 mL Canadian standard freeness (CSF) by the standard method T200 sp-01 (TAPPI 2001). NaOH and urea were purchased from Nanjing Chemical Reagent Co., Ltd. The thiourea was purchased from Shanghai Lingfeng Chemical Reagent Co., Ltd. The analytical grade NaOH, urea, and thiourea were used as received.

Methods

NFs preparation

The calculated amount of cellulose pulp was dispersed into the 100 g pretreatment system, which was precooled to -10 °C. In the pretreatment system, the weight ratio of NaOH:thiourea:urea:H₂O was equal to 7:9:9:75 (Wang *et al.* 2008). The solution was then ultrasonicated (sonication details are discussed in Results and Discussion), followed by centrifugation at 4000 rpm for 10 min. The supernatant liquid was continuously dialyzed against water until the dispersion reached a pH of 7. Subsequently, this precipitate was re-dispersed in water by ultrasonication to obtain NFs suspensions. The obtained NFs suspensions were freeze dried and used for further characterization. The NFs yield was defined as the weight of the oven dried NFs divided by the original weight of the cellulose,

$$Y = \frac{W_n}{W_p} \times 100\% \quad (1)$$

where Y is the NFs yield, W_n is the weight of the NFs, and W_p is the weight of the cellulose pulp. Each yield was obtained based on three parallel experiments. While the supernatant liquid was dialyzed against water, the sediment was collected for homogenization to obtain NFs-H. The sediment fibers were diluted to pH=14 and then homogenized 10 times by a high pressure homogenizer (EF-C3) at pressure levels ranging from 100 to 1000 bar.

Characterization

Thermogravimetric analysis (TG) was used to measure the thermal stability of the NFs (DTG-60AH). The experimental parameters used for TG included a heating rate of 10 K/min, a temperature range from room temperature to 600 °C, and a N₂ purging gas flow rate of 50 mL/min.

The crystalline structure of the fibers was analyzed by wide-angle X-ray

diffraction (XRD) on a Rigaku-D/MAX instrument (Ultima IV, Japan). Ni-filtered Cu-K α radiation generated at a voltage of 30 kV and a current of 30 mA with a scan speed of 3°/min from 5° to 40° was used. The degree of crystallinity was calculated according to the peak separation method (Zhang *et al.* 2009). The transmittance of the nanopaper was obtained with a UV-vis spectrometer (Lambda 35, PerkinElmer, USA).

Morphological analysis of raw fibers was done by scanning electron microscopy (SEM, JEM-1400 Japan). SEM micrographs of the fibers' surfaces were taken at voltage of 20 kV. Prior to SEM evaluation, the samples were gold coated, using a sputter coating apparatus. NFs lengths and widths were measured directly from transmission electron micrographs (TEM, FEI QUANTA 200 American). A drop of 10 μ L diluted NFs suspension was deposited onto glow-discharged carbon-coated TEM grids and the excess liquid was then removed after 2 min by blotting with filter paper. The samples were observed at a 100 kV accelerating voltage. The optical microscope images of the cellulose solution were determined by pipetting 50 μ L of the solution onto a clean glass slide and then covering it with cover glass to form a middle liquid layer of cellulose solution. Then, the samples were measured by a polarized optical microscope (POM) (Leica DM1000) at room temperature.

RESULTS AND DISCUSSION

Morphology of NFs

The raw fibers used in this paper were softwood fibers with diameters of approximately 50 μ m, as shown in Fig. 2a.

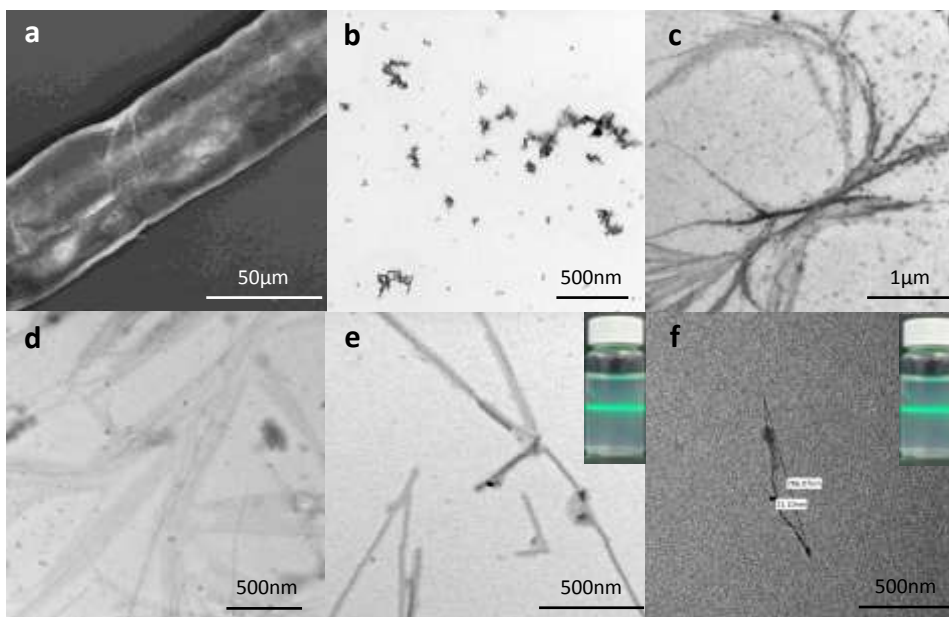


Fig. 2. SEM images of (a) raw cellulose fiber. TEM images of (b) NaOH, urea and thiourea CCP, (c) typical fiber in dissolving system, (d) loose NFs pack, uniformly dispersed in the dissolving system after sonication, (e) NFs obtained after dialyzed against distilled water, and (f) the NFs obtained from precipitate after homogenization. The inset pictures in (e) and (f) are NFs solutions under green laser beam.

In the pretreatment system, NaOH, urea, and thiourea formed complex compound particles (CCP), which can be seen in the TEM image in Fig. 2b. A similar observation was found in the work of Cai *et al.* (2008). When the cellulose fibers were added into the pretreating system, the CCP opened the chain packing of the cellulose through the formation of new hydrogen bonds between the cellulose and the CCP (Fig. 2c). The fibers were cleaved into small fibers, having part of their dimensions on the nanoscale, as shown in Fig. 2c. Ultrasonic treatment was applied to further disrupt cellulose chain packing, increasing the yield of NFs. After ultrasonication, the cellulose solution was centrifuged. The supernatant liquid was collected to take the TEM image shown in Fig. 2d. Figure 2d clearly shows that a large cellulose pack was loosened. After they were dialyzed against water, the NFs were approximately 30 nm in diameter while the length varied from 200 nm to several micrometers, as shown in Fig. 2e. The sediment after centrifugation was collected for further homogenization. After homogenization, the sediment was disintegrated into NFs-H (Fig. 2f). A green laser beam path formed in the NFs solutions, as shown in the inset pictures in Fig. 2e and 2f, respectively, which means that the solutions were in the colloid state.

X-ray Diffraction Analysis of NFs

The X-ray diffractograms of the raw materials, NFs and NFs-H, are shown in Fig. 3. The raw materials present cellulose crystal I form. However, the diffractograms for NFs and NFs-H clearly show cellulose crystal II form with peaks at about $2\theta=12$, 20, and 22.8 in the WXR patterns. These peaks are characteristics for cellulose II with the crystal planes of $(1\bar{1}0)$, (110) , and (200) .

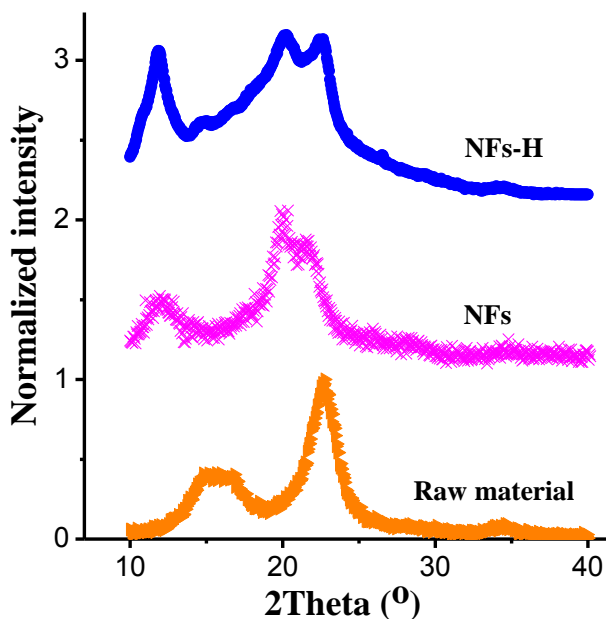


Fig. 3. X-ray diffractograms of raw material, NFs and NFs-H

The crystalline area dramatically decreased after the raw fiber was dispersed in the system. This effect was due to the strong interaction between cellulose and CCP, which can cleave the chain packing of cellulose and thus damage the crystal structure. The crystal structure change can be seen from the polarized optical images of fibers

before and after pretreatment in Fig. 4. In this work, the crystallinity of the NFs and NFs-H was 54.9% and 43.7%, respectively; this is lower than that of the untreated cellulose, which was 60.7%. That was due to the pretreatment and homogenization of the cellulose. During pretreatment and homogenization, the chain packing of the cellulose was cleaved, forming an amorphous phase (Jin *et al.* 2007). Although the cellulose II crystal structure was formed when the solution was dialyzed against water, the regenerated cellulose had lower crystallinity compared to raw cellulose.

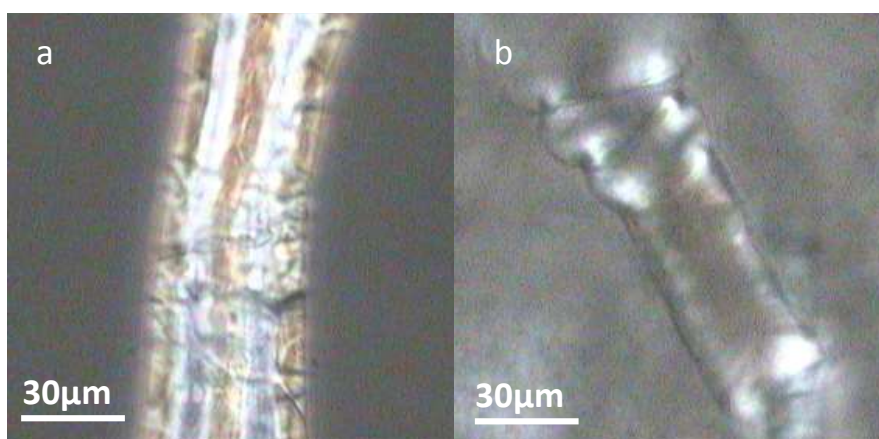


Fig. 4. Typical polarized optical images of (a) raw material fibers and (b) fibers in the pretreatment system

Thermal Properties of the NFs

The high thermal stability of the obtained NFs can broaden the field of NFs applications. Figures 5a and 5b show the TG and derivative curves of the isolated raw material fibers, NFs, and NFs-H. The TG curve shows an initial small weight loss before 120 °C, which corresponds to a mass loss of approximately 5% due to absorbed moisture. The onset temperature of degradation, which mostly restricts the application of NFs, are observed at 270 °C, 266 °C, and 250 °C for NFs, raw material fibers, and NFs-H, respectively. The DTG peak, accounting for the maximum degradation temperature of cellulose, are observed at around 370 °C, 358 °C, and 335 °C, respectively (Chen *et al.* 2011). The thermal stability of NFs here is better than NFs obtained from acid hydrolysis of cotton cellulose (onset temperature is about 150 °C, maximum degradation temperature < 300 °C) (Lu and Hsieh 2010), neutralized NFs by acid hydrolysis of bacterial cellulose (onset temperature is about 212 °C, maximum degradation temperature is 332 °C) (Martinez-Sanz *et al.* 2011), NFs made by homogenization of ionic liquid treated sugarcane bagasse (onset temperature is about 200 °C, maximum degradation temperature is 238 °C) (Li *et al.* 2012), and NFs made by TEMPO oxidation of rice straw cellulose (onset temperature is about 210 °C, maximum degradation temperature is 265 °C) (Jiang and Hsieh 2013). Note that all the data were obtained by TG with a heating rate of 10 K/min under N₂ purging gas flow. The thermal stability of the produced NFs was even higher than that of raw material fibers. The high thermal stability here mainly can be attributed to the cellulose II crystal form and the high crystallinity. The chains in cellulose II are in an antiparallel arrangement. This arrangement yields more hydrogen bonds, leading to a more stable structure compared to other polymorphs (Kovalenko 2010). The high thermally stable NFs obtained have potential applications on high thermally stable

organic transistors for medical applications and separators for lithium-ion batteries (Chun *et al.* 2012; Huang *et al.* 2013; Kuribara *et al.* 2012). The onset temperature and the maximum degradation temperature of NFs-H were both lower than that of the NFs and the raw material fibers. These temperatures were mainly due to the low crystallinity of NFs-H. For the low thermal stable NFs-H, they can be used to make transparent paper (Zhu *et al.* 2013). The transmittance of the paper made from NFs-H is 90% at the wavelength of 550 nm.

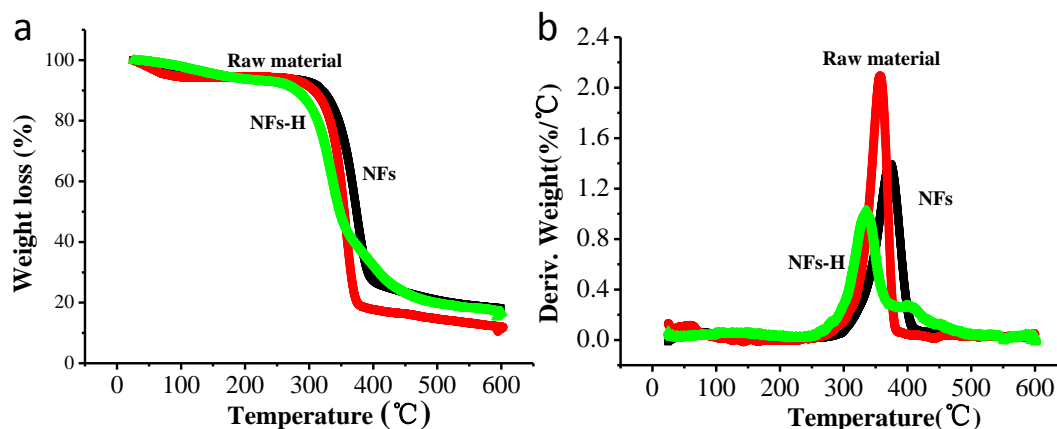


Fig. 5. TG (a) and DTG (b) curves of raw material fibers, NFs, and NFs-H. Red line is referred to raw material fibers, black line is referred to NFs, and green line is referred to NFs-H.

Effects of Pre-cool Temperature and Ultrasonic Energy on NFs Yields

The process of cellulose dissolution in this system is exothermic, and the strong hydrogen-bonded networks, formed by CCP, occur more easily at low temperature than at high temperature (Zhang *et al.* 2010). Figure 6 shows that the pretreatment of cellulose was favored by low temperature. However, when the temperature was -18°C , part of the CCP precipitated out of the solution, which hindered cellulose pretreatment (Zhang *et al.* 2010). In order to determine the influence of pretreatment on the NFs preparation, cellulose treated only by sonication was made as a control sample (sonication power was 500 W, time was 30 min, cellulose concentration was 0.5%). However, the obtained suspension was the same as a regular fiber suspension. SEM images of the fiber were also taken to show that the fibers were the same shape and diameter as raw cellulose fiber (Fig. 6c). Note that the surface appears cracked, which means that ultrasonication can break up the cellulose wall.

Ultrasonic energy has often been applied for the dispersion of nanoparticles. When high intensity ultrasound is applied, cavitation bubbles develop and grow. A large amount of energy is released from the collapse of these bubbles, creating a mechanical shock wave effect and leading to the disruption of particle agglomerates (Bittmann *et al.* 2009). NFs were obtained by a combination of pretreatment and sonication. When low sonication power was applied, only the weak bonds could be broken. Thus, pretreatment played the dominant role in obtaining NFs. When the applied power was high, strong bonds could be broken up by sonication. In this case, sonication was the dominant role in making NFs. That is why the NFs yield difference between a pretreatment temperature of -10°C and -18°C decreased when the sonication power was larger than 300 W. The yield of NFs increased with higher ultrasonic energy introduction. When the power

reached 500 W, the highest yield was obtained for pretreatment under each of the four temperatures employed in this study.



Fig. 6. (a) Effects of pre-cool temperature and ultrasonic energy on NFs yields, when the ultrasonic time was set at 30 min (1 s pause every 2 s sonication), and the cellulose concentration was 2%; (b) SEM image of ultrasonication treated cellulose; (c) Effects of cellulose concentration on NFs yield, when the pre-cool temperature was $-10\text{ }^{\circ}\text{C}$, the ultrasonic energy was 500 W, and the ultrasonic time was 30 min.

Effects of Cellulose Concentration on NFs Yields

The higher the concentration of cellulose, the more viscous the system was. The initiation of the cavitation process requires more energy in a viscous system, thus more energy was required to break cellulose chains. When the cellulose concentration was 0.5%, the NFs yield was 85.4%. However, the NFs yield decreased to 35.5% at a cellulose concentration of 2.5% (Fig. 5b). It can be concluded that lower concentrations favor swollen and defibrillated fibers in the solvent. When the cellulose concentration was increased to 2.5%, the solution was so viscous that it was difficult for it to be dispersed uniformly by ultrasonication. Since the solvent has the ability to swell and “dissolve” cellulose, the NFs yield was still 34.7% at a cellulose concentration of 3.0%, despite the higher viscosity.

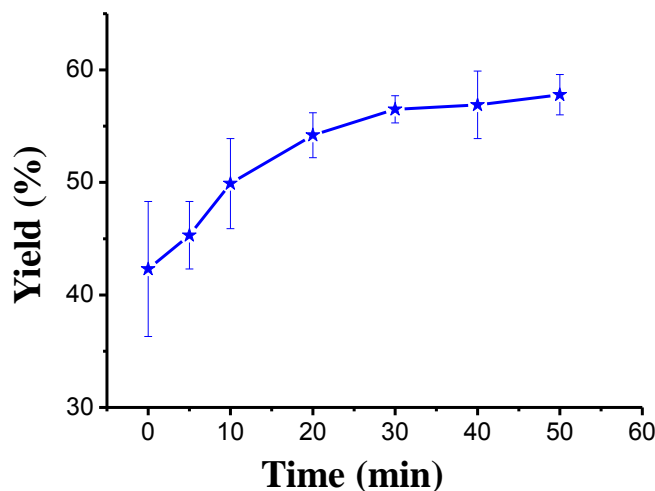


Fig. 7. Effects of ultrasonic time on the NFs yield; when the pre-cool temperature was $-10\text{ }^{\circ}\text{C}$, the ultrasonic energy was 500 W, and the cellulose concentration was 2%

Effects of Ultrasonic Time on NFs Yields

Time dictates the quality of the dispersion. Longer sonication time is better for the preparation of NFs with high yield. Besides the yield increase, this also leads to shorter NFs with smaller diameter (Frone *et al.* 2011). If the sonication time is too long, more NFs will be broken, and this may change the morphology of nanofibers into nanowhiskers. Compared with a sample without sonication treatment, the NFs yield increased from 42.3% to 56.5% after 30 min of sonication (Fig. 7). When the ultrasonic time was prolonged to 50 min, there was only a 2.3% increase in the yield. Therefore, 30 min of sonication is enough for sufficient dispersion of NFs.

CONCLUSIONS

Cellulose II NFs with a high yield were obtained by first pretreating the raw cellulose in NaOH/urea/thiourea solution, and then defibrillating the fibers through ultrasonication. The unfibrillated celluloses were collected for homogenization to obtain NFs-H. The optimal parameters for the NFs preparation are a pre-cool temperature of -10 °C, an ultrasonic energy of 500 W, and an ultrasonic time of 30 min with a cellulose concentration of 0.5%. The obtained NFs are 30 nm in diameter with lengths ranging from hundreds of nanometers to micrometer. They are also in cellulose II crystal form with high thermal stability. The onset of thermal degradation is 270 °C, and the maximum degradation temperature is 370 °C. The high yield and thermal stability broaden the possible applications of NFs. The high thermal stability of nanocellulose has potential application in making thermally stable films for transistors and batteries. NFs-H was also in cellulose II crystal form but with lower thermal stability due to the low crystallinity. It can be applied to make transparent paper.

ACKNOWLEDGMENTS

We are grateful for the support from the Priority Academic Program Development of Jiangsu Higher Education Institutions (PAPD), the Graduate Student Innovation Program of Jiangsu Province (CXLX12_0531), and the Nanjing Forestry University Innovation fund program for the Doctorate Fellowship Foundation. We acknowledge Kathleen Rohrbach for the grammar check of this paper.

REFERENCES CITED

- Beck-Candanedo, S., Roman, M., and Gray, D. G. (2005). "Effect of reaction conditions on the properties and behavior of wood cellulose nanocrystal suspensions," *Biomacromolecules* 6, 1048-1054.
- Bittmann, B., Hauptert, F., and Schlarb, A. K. (2009). "Ultrasonic dispersion of inorganic nanoparticles in epoxy resin," *J. Ultrasonics Sonochemistry* 16, 622-628.
- Bondeson, D., Mathew, A., and Oksman, K. (2006). "Optimization of the isolation of nanocrystals from microcrystalline cellulose by acid hydrolysis," *Cellulose* 13, 171-180.

- Cai, J., Zhang, L., Liu, S. L., Liu, Y. T., Xu, X. J., Chen, X. M., Chu, B., Guo, X. L., Xu, J., Cheng, H., Han, C. C., and Kuga, S. (2008). "Dynamic self-assembly induced rapid dissolution of cellulose at low temperatures," *J. Macromolecules* 41, 9345-9351.
- Chen, W. S., Yu, H. P., Liu, Y. X., Hai, Y. F., Zhang, M. X., and Chen, P. (2011). "Isolation and characterization of cellulose nanofibers from four plant cellulose fibers using a chemical-ultrasonic process," *Cellulose* 18, 433-442.
- Chun, S. J., Choi, E. S., Lee, E. H., Kim, J. H., Lee, S. Y. (2012). "Eco-friendly cellulose nanofiber paper-derived separator membranes featuring tunable nanoporous network channels for lithium-ion batteries," *J. Journal of Materials Chemistry* 22, 16618-16626.
- Fox, J., Wie, J. J., Greenland, B. W., Burattini, S., Hayes, W., Colquhoun, H. M., Mackay, M. E., and Rowan, S. J. (2012). "High-strength, healable, supramolecular polymer nanocomposites," *Journal of the American Chemical Society* 134, 5362-5368.
- Frone, A. N., Panaitescu, D. M., Donescu, D., Spataru, C. I., Radovici, C., Trusca, R., and Somoghi, R. (2011). "Preparation and characterization of PVA composites with cellulose nanofibers obtained by ultrasonication," *BioResources* 6(1), 487-512.
- Habibi, Y., Lucia, L. A., and Rojas, O. J. (2010). "Cellulose nanocrystals: Chemistry, self-assembly, and applications," *Chemical Reviews* 110, 3479-3500.
- Henriksson, M., Henriksson, G., Berglund, L. A., and Lindstrom, T. (2007). "An environmentally friendly method for enzyme-assisted preparation of microfibrillated cellulose (MFC) nanofibers," *European Polymer Journal* 43, 3434-3441.
- Hu, L. B., Zheng, G. Y., Yao, J., Liu, N. A., Weil, B., Eskilsson, M., Karabulut, E., Ruan, Z. C., Fan, S. H., Bloking, J. T., McGehee, M. D., Wagberg, L., and Cui, Y. (2013). "Transparent and conductive paper from nanocellulose fibers," *J. Energy & Environmental Science* 6, 513-518.
- Huang, J., Zhu, H. L., Chen, Y. C., Preston, C., Rohrbach, K., Cumings, J., and Hu, L. B. (2013). "Highly Transparent and Flexible Nanopaper Transistors," *J. ACS Nano* 7, 2106-2113
- Isogai, A., Saito, T., and Fukuzumi, H. (2011). "TEMPO-oxidized cellulose nanofibers," *J. Nanoscale* 3, 71-85.
- Jiang, F., and Hsieh, Y. L. (2013). "Chemically and mechanically isolated nanocellulose and their self-assembled structures," *J. Carbohydrate Polymers* 95, 32-40.
- Jin, H. J., Zha, C. X., and Gu, L. X. (2007). "Direct dissolution of cellulose in NaOH/thiourea/urea aqueous solution," *J. Carbohydrate Research* 342, 851-858.
- Korhonen, J. T., Hiekkataipale, P., Malm, J., Karppinen, M., Ikkala, O., and Ras, R. H. A. (2011). "Inorganic hollow nanotube aerogels by atomic layer deposition onto native nanocellulose templates," *J. ACS Nano* 5, 1967-1974.
- Kovalenko, V. I. (2010). "Crystalline cellulose: Structure and hydrogen bonds," *Russian Chemical Reviews* 79, 231-241.
- Kuribara, K., Wang, H., Uchiyama, N., Fukuda, K., Yokota, T., Zschieschang, U., Jaye, C., Fischer, D., Klauk, H., Yamamoto, T., Takimiya, K., Ikeda, M., Kuwabara, H., Sekitani, T., Loo, Y. L., and Someya, T. (2012). "Organic transistors with high thermal stability for medical applications," *J. Nature Communications* 3, 723.
- Lavoine, N., Desloges, I., Dufresne, A., and Bras, J. (2012). "Microfibrillated cellulose - Its barrier properties and applications in cellulosic materials: A review," *J. Carbohydrate Polymers* 90, 735-764.

- Li, J. H., Wei, X. Y., Wang, Q. H., Chen, J. C., Chang, G., Kong, L. X., Su, J. B., Liu, and Y. H. (2012). "Homogeneous isolation of nanocellulose from sugarcane bagasse by high pressure homogenization," *J. Carbohydrate Polymers* 90, 1609-1613.
- Li, W., Wang, R., and Liu, S. X. (2011). "Nanocrystalline cellulose prepared from softwood kraft pulp via ultrasonic-assisted acid hydrolysis," *BioResources* 6(4), 4271-4281.
- Li, Y., and Dai, H. Q. (2012). "Preparation of nano-crystalline cellulose by chemical methods," *Journal of Nanjing Forestry University(Natural Science Edition)* 36, 161-166.
- Li, Y. Y., Zhu, H. L., Gu, H. B., Dai, H. Q., Fang, Z. Q., Weadock, N. J., Guo, Z. H., and Hu, L. B. (2013). "Strong transparent magnetic nanopaper prepared by immobilization of Fe₃O₄ nanoparticles in a nanofibrillated cellulose network," *J. Journal of Materials Chemistry A* 1, 15278-15283.
- Lu, P., and Hsieh, Y. L. (2010). "Preparation and properties of cellulose nanocrystals: Rods, spheres, and network," *J. Carbohydrate Polymers* 82, 329-336.
- Martinez-Sanz, M., Lopez-Rubio, A., and Lagaron, J. M. (2011). "Optimization of the nanofabrication by acid hydrolysis of bacterial cellulose nanowhiskers," *Carbohydrate Polymers* 85, 228-236.
- Martins, M. A., Teixeira, E. M., Correa, A. C., Ferreira, M., and Mattoso, L. H. C. (2011). "Extraction and characterization of cellulose whiskers from commercial cotton fibers," *Journal of Materials Science* 46, 7858-7864.
- Mishra, S. P., Thirree, J., Manent, A. S., Chabot, B., and Daneault, C. (2011). "Ultrasound-catalyzed TEMPO-mediated oxidation of native cellulose for the production of nanocellulose: effect of process variables," *BioResources* 6(1), 121-143.
- Montanari, S., Rountani, M., Heux, L., and Vignon, M. R. (2005). "Topochemistry of carboxylated cellulose nanocrystals resulting from TEMPO-mediated oxidation," *Macromolecules* 38, 1665-1671.
- Nogi, M., Iwamoto, S., Nakagaito, A. N., and Yano, H. (2009). "Optically transparent nanofiber paper," *J. Advanced Materials* 21, 1595-1598.
- Sadeghifar, H., Filpponen, I., Clarke, S. P., Brougham, D. F., and Argyropoulos, D. S., (2011). "Production of cellulose nanocrystals using hydrobromic acid and click reactions on their surface," *Journal of Materials Science* 46, 7344-7355.
- Spence, K. L., Venditti, R. A., Rojas, O. J., Habibi, Y., and Pawlak, J. J. (2011). "A comparative study of energy consumption and physical properties of microfibrillated cellulose produced by different processing methods," *Cellulose* 18, 1097-1111.
- Tang, L. R., Huang, B., Ou, W., Chen, X. R., and Chen, Y. D. (2011). "Manufacture of cellulose nanocrystals by cation exchange resin-catalyzed hydrolysis of cellulose," *Bioresource Technology* 102, 10973-10977.
- Tejado, A., Alam, M. N., Antal, M., Yang, H., and van de Ven, T. G. M. (2012). "Energy requirements for the disintegration of cellulose fibers into cellulose nanofibers," *Cellulose* 19, 831-842.
- Wang, H. F., Zhu, P., Zhang, and C. J. (2008) "Dissolution of cellulose in NaOH/urea/thiourea aqueous solution," *J. Synthetic Fiber in China* 37, 28-32.
- Wang, Q. Q., Zhu, J. Y., Reiner, R. S., Verrill, S. P., Baxa, U., and McNeil, S. E. (2012). "Approaching zero cellulose loss in cellulose nanocrystal (CNC) production:

- recovery and characterization of cellulosic solid residues (CSR) and CNC," *Cellulose* 19, 2033-2047.
- Yan, L. F., and Gao, Z. J. (2008). "Dissolving of cellulose in PEG/NaOH aqueous solution," *Cellulose* 15, 789-796.
- Yue, Y. Y. (2011). "A Comparative study of cellulose I and II fibers and nanocrystals," *D*, Louisiana State University
- Zhang, S. A., Li, F. X., Yu, J. Y., and Hsieh, Y. L. (2010). "Dissolution behaviour and solubility of cellulose in NaOH complex solution," *Carbohydrate Polymers* 81, 668-674.
- Zhang, S. A., Li, F. X., Yu, J. Y., Gu, L. X. (2009). "Novel fibers prepared from cellulose in NaOH/thiourea/urea aqueous solution," *J. Fibers and Polymers* 10, 34-39.
- Zhu, H. L., Parvinian, S., Preston, C., Vaaland, O., Ruan, Z. C., and Hu, L. B. (2013). "Transparent nanopaper with tailored optical properties," *Nanoscale* 5, 3787-3792.
- Zhu, H. L., Xiao, Z. G., Liu, D. T., Li, Y. Y., Weadock, N. J., Fang, Z. Q., Huang, J. S., and Hu, L. B. (2013). " Biodegradable transparent substrates for flexible organic-light-emitting diodes," *Energy & Environmental Science* 6, 2105-2111.

Article submitted: July 20, 2013; Peer review completed: September 9, 2013; Revised version received: December 26, 2013; Second revision: January 8, 2014; Third revision received and accepted: February 12, 2014; Published: February 18, 2014.